

Application of electrical capacitance tomography and artificial neural networks to rapid estimation of cylindrical shape parameters of industrial flow structure

HELA GARBAA^{1,2}, LIDIA JACKOWSKA-STRUMILLO¹, KRZYSZTOF GRUDZIEN¹,
ANDRZEJ ROMANOWSKI¹

¹*Lodz University of Technology, Institute of Applied Computer Science
Siefanowskiego, 18/22, 90-924, Łódź, Poland
tel +48 426312750, fax +48 426312755
e-mail: lidia_js@kis.p.lodz.pl; helagarbaa@gmail.com
kgrudzi@kis.p.lodz.pl; androm@kis.p.lodz.pl*

²*REsearch Groups in Intelligent Machines (REGIM-Lab)
University of Sfax, National School of Engineers (ENIS)
BP 1173, Sfax 3038, Tunisia*

(Received: 03.11.2015, revised: 14.09.2016)

Abstract: A new approach to solve the inverse problem in electrical capacitance tomography is presented. The proposed method is based on an artificial neural network to estimate three different parameters of a circular object present inside a pipeline, i.e. radius and 2D position coordinates. This information allows the estimation of the distribution of material inside a pipe and determination of the characteristic parameters of a range of flows, which are characterised by a circular objects emerging within a cross section such as funnel flow in a silo gravitational discharging process. The main advantages of the proposed approach are explicitly: the desired characteristic flow parameters are estimated directly from the measured capacitances and rapidity, which in turn is crucial for online flow monitoring. In a classic approach in order to obtain these parameters in the first step the image is reconstructed and then the parameters are estimated with the use of image processing methods. The obtained results showed significant reduction of computations time in comparison to the iterative LBP or Levenberg-Marquard algorithms.

Key words: artificial neural networks, electrical capacitance tomography, flow parameters estimation, inverse problem

1. Introduction

Process monitoring consists in resolving the internal state of the system and ensuring that the process remains under the appropriate conditions and proceeds in a correct manner. Espe-

cially online monitoring, which allows the process control in real time, is demanded in various industrial processes. For example online monitoring of the gravitational solids flow parameters prevents possible unwanted phenomena and dangerous breakdowns as well as ensures a good quality of industrial products [1, 19]. The researchers are still working on the development of new technologies for acquiring more valuable information about the process states during production. Such a situation requires robust technologies, which are able to provide information about the changes of the characteristic parameters of an industrial process in real time. For the online industrial process monitoring, high speed techniques are demanded, which allow to visualize the process in real time, providing a lot of information about the process state in spatial-temporal changes context [21]. One of technologies, which can meet with these challenges, is process tomography. The process tomography is a useful technique, which provides a cross sectional 2D or 3D visualization of the material distribution inside a vessel by sensing, analysing and interpreting specific measurements. The procedure, which allows the visualisation of the material distribution inside sensor's space in a form of an image, is called the image reconstruction procedure. From a mathematical point of view it is so called the inverse problem solving, which solution gives information about the material distribution inside a vessel in a form of an image [9] or in a form of a set of process parameters [9, 24, 20], on the basis of the measurement records.

From the practical point of view the tomography measurement unit works on different physical rules. Authors in [9] reviewed non-invasive process tomography techniques used to monitor chemical mixture: X-ray computed tomography, ultrasonic tomography, optical tomography, electrical capacitance tomography and electrical resistance tomography. Each of tomography modalities is characterized by different speed of an acquisition module and spatial resolution of reconstructed images. The proper choice of tomography type at first is conditioned by dynamics of process monitoring, and then by cost and robustness of the system. According to the dependency of the sensitivity of the distribution inside the vessel on measurements, tomography techniques are classified into hard- or soft-field non-invasive techniques [20]. This division comes from the influence on measured signal strength by material present within the measurement space. In the case of hard field tomography systems material distribution attenuates a measurement signal however does not modify the path it is travelling along. In the case of the soft-field tomography the material distribution inside the sensor space may alter the path of the measurement signal on its way between the source and the detector. It can be said, that sensitivity of measurements is dependent on the material distribution in sensor space, which is significant during image reconstruction procedure for electrical tomography. Additional difficulties of soft field types of tomography (especially electrical tomography), from a practical point of view, concern underdetermined and ill-conditioned properties of the inverse problem. Real time applications enforce a smaller number of measurements, which cause the under determination of the problem, when the number of pixels in the reconstructed image is much higher than the records. The other aspect, i.e. ill-conditioned nature means big changes in the distribution of material inside the sensor may cause small changes in measurements.

The methodology presented in this paper, solving an inverse problem, was proposed for Electrical Capacitance Tomography (ECT). This type of tomography is often used for visualisation of multiphase flow [14]. ECT has been especially widely applied to process monitoring and measuring particulate distribution, to identify flow regime and to detect chemical mixtures [2, 6, 7]. It is also considered the most highly performing technique for visualizing fluidised bed granulation and drying processes [19] and also for the silo flow and bulk solid pulsation detection [1]. The main advantages of ECT systems are high speed data acquisition and robustness.

The ECT is sensitive to changes in the electrical permittivity distribution (related to material density), which allows tracking of phenomena taken place during the process, providing realistic information about the process state [20]. In most modalities, especially in ECT, the speed of an acquisition system fulfils with excess the industrial requirements. In this case the main problem is data analysis in real time to receive important information about the process states and a quality level of the obtained information. In the case of a reconstructed image it concerns the spatial resolution. Current state of art, concerning ECT application, shows that the most important aspect in developing of ECT tomography is the improvement of the quality level of the obtained information about the process in real time. In order to meet this challenge, new artificial intelligence techniques e.g. fuzzy logic [16] and Artificial Neural Network (ANN) [18, 23].

Authors are developing a new method of rapid estimation of important parameters of the process, characterised by the cylindrical flow structure, using electrical capacitance tomography and artificial neural networks. ANNs are universal approximators and an effective tool for solving a complex non-linear problem [22]. ANNs were successfully applied to similar shape inverse problem solving and image reconstruction using electrical impedance tomography [3, 15, 17]. Coupled with principal component analysis, the ANN method provided a real time solution of the Electrical Impedance Tomography (EIT) inverse problem [15]. In the proposed approach ANN is trained to determinate the radius and position of a circular object present inside a pipeline using ECT. The network training is a laborious and time-consuming process, but once trained ANN can be used many times for rapid and direct estimation of the desired flow parameters directly from the measured capacitances. The proposed technique can be applied for example for online monitoring of gravitational flow of solids. In this case, the radius and the position of a funnel are crucial process parameters.

2. Electrical capacitance tomography

Electrical capacitance tomography is a technique enabling the visualisation of the distribution of a mixture of materials with different dielectric properties (permittivity) flowing inside a pipe or a vessel [4]. ECT relies on measuring the capacitances between pairs of electrodes placed around the targeted vessel. The acquired measurements are then processed to reconstruct a tomographic image by the use of an appropriate image reconstruction algorithm, which is the so called inverse problem solving. The spatial distribution of the materials present

inside the isolated vessel is determined. This technique has the advantages to be a non-invasive and non-destructive tool to measure and monitor processes in hazardous or unreachable areas (high temperature, high pressure). Comparing to other tomography modalities, ECT is low cost and fast. Disadvantage of this technique lies in the poor resolution of the provided image. Researchers are still investigating how to improve the performance of this technique and agree on the complexity of the task due to the difficulties with the inverse problem solution. Two major characteristic obstacles of the inverse problem are: its ill-posed and non-linear properties. The first refers to the limited number of measured capacitances compared to the number of pixels to be reconstructed while the non-linear relationship between capacitance and permittivity distribution is modelled by the Gauss Law, [8, 9], (Eq. 1):

$$C = \frac{Q}{V} = -\frac{1}{V} \iint_{\Gamma} \epsilon(x, y) \nabla \varphi(x, y) \cdot d\Gamma, \quad (1)$$

where: Q is the electric charge, V is the potential difference between two electrodes, $\epsilon(x, y)$ denotes the permittivity distribution and $\varphi(x, y)$ represents the electrical potential distribution. Γ is the electrode surface and $d\Gamma$ an element orthogonal to this surface.

A discrete linear approximation of the previous equation is formulated as following (Eq. 2):

$$C = S\epsilon, \quad (2)$$

where: C is a vector of measured capacitances, S is the linearized sensitivity matrix and ϵ is a vector of permittivity distribution. The problem of image reconstruction is then reduced to solving the linear discrete form (3):

$$\epsilon = S^{-1}C, \quad (3)$$

The challenge in solving Eq. 3 can be described as: The inverse of S does not exist; because S is not a square matrix (number of measurements is not equal to the number of pixels in an image). Instead of having its inverse S^{-1} , the pseudo-inverse S^* can be calculated. The other important problem in image reconstruction procedure is the dependence of the sensitivity matrix on the permittivity distribution, which causes that the inverse problem is non-linear. Different kinds of methods for the inverse problem solving (linear, non-linear, direct methods and iterative methods) are presented in the literature [10]. Depending on a computational method, the algorithm generates images with different levels of quality. In the case of iterative and non-linear methods high image quality requires a long computational time. However progress in parallel computing with aid of GPU units in recent years allows the reduction of the computation time of the inverse problem solutions [11]. The artificial neural network constitutes a competitive optimisation based method applied in the same research era [10, 23].

For control purposes, only a determination of important process parameters is demanded. With a parameterization the process interpretation is simplified and the inverse problem is better posed. Such an approach can be found e.g. in [5] where four fundamental process parameters were measured to online assess the quality of a given product.

In this paper, a new approach using artificial neural networks is proposed to solve the inverse problem and estimate three characteristic shape parameters: radius r and position co-

ordinates (x, y) of a cylindrical structure present inside a vessel. Such a structure is observed during a gravitational silo discharging process or gas-liquid flow, where material in some part of the vessel cross-section characterises lower concentration and geometry of this area takes a cylindrical shape.

3. Gravitational flow of granular

Gravitational silo discharging is a commonly used method applied at the storage granular material (corns, cements, etc.) and after unloading to other elements of flow installation or to the receiving terminal equipment. The behaviour of material during the silo discharging process depends on granular properties and also silo construction [13, 24]. Two main types of flow are distinguished: mass flow, where material is moving with the same velocity in the whole cross-section of a silo, and funnel flow, where material is moving only in the central part of the cross-section [13]. In both situations unwanted phenomena can happen. In this paper, the presented approach concerns the funnel flow. For this silo discharging type the most unwanted phenomena are arching (blocked funnel – stopping discharging process), rat holing (empty funnel – stopping discharging process). To avoid these situations the funnel area should be monitored. The movement of material in the central part of the cross-section container is distinguished by a lower packing of the material than in its other areas (Fig. 1). This area is called funnel flow and is characterized by changes in shape and size during silo discharging.

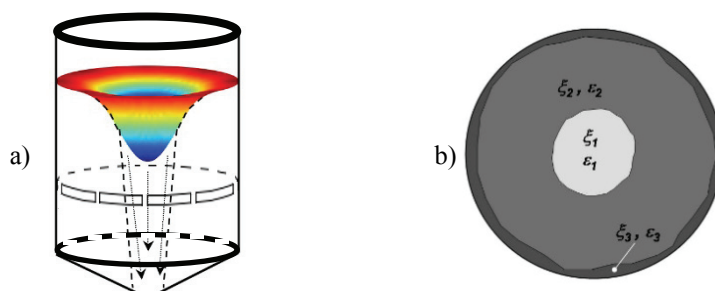


Fig. 1. Geometrical model of the silo, a) a simplified diagram of emptying the silo-funnel flow, b) the cross sectional area of the silo (ξ_1, ϵ_1 – parameters of funnel; size, material concentration) [24]

The next figure presents reconstructed images for funnel flow for a partial blockage of the silo. The blockage was prepared before filling the silo. Such set-up of silo construction enforced shift of the funnel area from the centre position as for normal flow, without the blockage (Fig. 2a). Based on these results it was concluded, that tracking of the funnel position is very useful to monitor a proper flow.

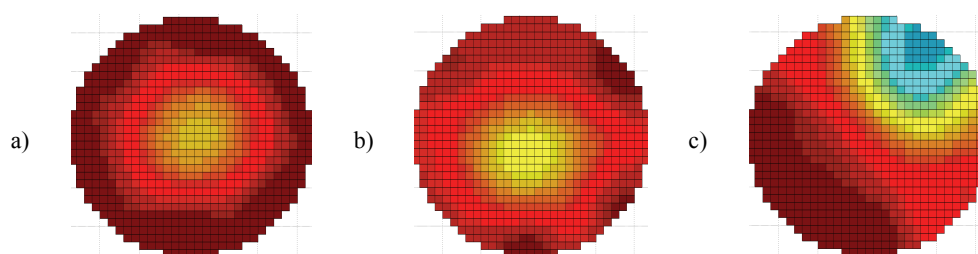


Fig. 2. Example of reconstructed image of funnel flow, a) material distribution without blockage of silo, b) material distribution with blockage of silo (blockage below ECT sensor), c) material distribution with blockage of silo (blockage above ECT sensor)

4. Artificial neural network and inverse problem solving

Artificial neural networks have been used for solving both forward and inverse ECT problems since they represent a powerful and effective tool to deal with complex and non-linear computations [22]. The type of the applied neural network differs depending on the purpose of investigations. A multilayer feed-forward neural networks was used in [12] to directly estimate the component fractions of material in multicomponent flows from ECT data.

An MLP (Multi-Layer Perceptron) was applied in [22] to identify the size and position of hidden objects in medical images and allowed real time image reconstruction.

In the current work, an MLP with one hidden layer and a sigmoidal transfer function was trained applying the back propagation algorithm performed the estimation of three shape parameters (r, x, y) of the flow from ECT data simulated using the ECTSim Matlab toolbox [26]. The ANN-based inverse model has been built on the basis of relations between the network input and output vectors. The knowledge about the inverse mapping is stored within the network structure and the network connection weights [3]. ANN needs to have an appropriate structure to deal with the complexity of the handled problem. A vector of sixty six values of capacitances $C = [C_1, \dots, C_{66}]$ constitute the network inputs. The approximated values of the corresponding radius and coordinates are calculated at the outputs. The number of hidden neurons has been determined experimentally. The back propagation learning algorithm was applied in order to adjust the synaptic weights of the network and generate the model that maps the input to the output using historical data called learning samples. The generalization properties of the ANN based model were checked by the cross validation method.

5. Proposed approach

The idea of flow parameters determination from ECT data is shown in Figure 3. In a traditional approach an appropriate image is at first reconstructed from the measurement data and then a processing algorithm is needed to interpret the provided image and extract the useful

information, e.g. flow parameters (Fig. 3a). An evaluation of existing reconstruction algorithms for different shapes and sizes of industrial flows is provided in [20].

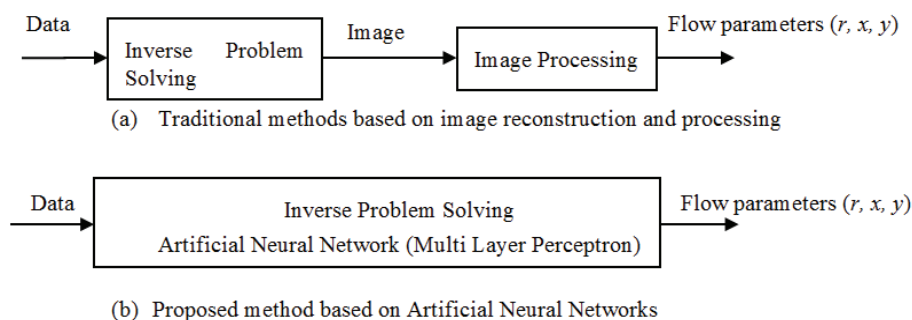


Fig. 3. Different approaches to determine the shape flow parameters from capacitances data: (a) traditional method, (b) the proposed ANN-based method

The proposed ANN-based approach solves the ECT inverse problem with no image processing step and allows obtaining the target information in a direct manner as shown in the scheme in Fig. 3b. The capacitance data is fed to the multi-layer perceptron at the input layer and the radius and position of the object are obtained at the output layer.

In the case of continuous changes of the size of the object inside a pipe, the precision of this parameter changes estimation is directly related to the quality of the reconstructed image, implemented image processing algorithm and time of computations. The proposed ANN based method of shape flow parameters determination provides a significant reduction of the time of computations.

In the previous work [18], MLP was trained to estimate the radius of a circular object placed in the centre of the silo. Efficient results were obtained. Computational time was reduced about 120 times comparing to the existing Landweber iterative algorithm. In the present paper, in addition to the size of the circular object inside the pipe, its position is also determined. Different structures of ANNs of the MLP type are tested for three parameters estimation: position (x, y) and radius (r) of the object.

6. Experimental part

Simulations described in this section were performed in MATLAB programming environment. Tomographic data used to train and test MLP was simulated via the ECTsim Matlab toolbox [26]. MATLAB functions were developed and implemented for ANN design and training. Different positions and radii of phantoms considered in the simulation are shown in the Fig. 4.

A sensor with 12 electrodes ($N = 12$) placed inside the pipe (inner insulator thickness = 0), background permittivity = 1 and elements' permittivity = 3 were considered. The field of view diameter was set to 84 mm. The sensor field of the view was then divided into 96×96 square

meshes. For each phantom the simulated capacitances were calculated using the discrete linear approximation of Gauss Law (Eq. 2). A set of ANN training data was generated using ECTsim Matlab toolbox for 990 different phantoms and then divided to 750 learning samples and 240 testing samples. The obtained data (a set of vectors of 66 capacitances) were provided to the ANN input layer. The network was trained to estimate the corresponding radius and position of a given phantom. A sum squared error cost function and backpropagation learning algorithm [22] was applied for the considered problem. These ensure that the convergence condition for the learning algorithm is true. In the present approach, the stop condition corresponds to a set value of the training error (TE).

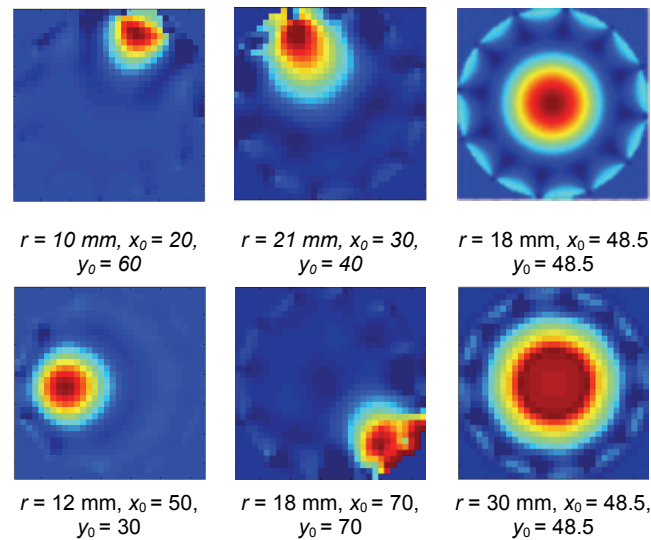


Fig. 4. Examples of different positions and different radii of phantoms considered in the simulation

The first aim of the research was to determine the appropriate MLP structure for different radii and centres' positions estimation. Different MLP structures (66- m -3), with 66 inputs, various numbers of neurones ($m = 10, 14, 20$ and 66) in the hidden layer and three neurones in the output layer were trained and tested (see the Table 1). The neurones in the hidden layer have a sigmoidal activation function, and these in the output layer have a linear activation function. More than 200 different MLPs were trained.

The main criterion for choosing the best MLP structure was the minimum of mean square error (MSE) for the testing data:

$$MSE = \frac{1}{n} \sum_{i=1}^n \|e_i(\mathbf{p})\|_2^2, \quad (4)$$

where: $\|\cdot\|_2$ means Euclidean norm, $e_i(\mathbf{p}) = \mathbf{p}_i - \tilde{\mathbf{p}}_i$, and \mathbf{p}_i corresponds to the desired set of parameters for i -th sample (x_i, y_i, r_i) , $\tilde{\mathbf{p}}_i$ denotes the corresponding estimated set of parameters at the MLP output and n is the number of testing samples.

In the selection of the appropriate MLP structure two other testing errors defined for each single shape parameter were also taken into consideration in addition to the MSE:

Root Mean Square Error (RMSE):

$$RMSE = \sqrt{\frac{1}{n} \sum_{i=1}^n e_i(p)^2} \tag{5}$$

Mean absolute error (ME):

$$ME = \frac{1}{n} \sum_{i=1}^n |e_i(p)|, \tag{6}$$

where: $e_i(p) = p_i - \tilde{p}_i$, and p_i corresponds to the desired single parameter $(x_i, y_i \text{ or } r_i)$ for i -th sample, \tilde{p}_i denotes the estimated parameter at MLP output and n the number of the testing samples.

The provided testing errors for a training error $TE = 0.12$ are gathered in Table 1. A structure (66-14-3) provided the most satisfactory testing errors and the smallest number of iterations in the learning process. This structure was maintained to further experiments.

Table 1. Testing errors and number of iterations with different MLP structures (training error $TE = 0.12$ corresponding to $MSE = 0.0003$)

Network structure	Testing error			Number of iterations (learning)
	MSE	RMSE $\begin{cases} r \\ x \\ y \end{cases}$	ME $\begin{cases} r \\ x \\ y \end{cases}$	
(66-10-3)	0.0541	$\begin{cases} 0.032 \\ 0.0463 \\ 0.0443 \end{cases}$	$\begin{cases} 0.0199 \\ 0.0290 \\ 0.0289 \end{cases}$	12631000
(66-14-3)	0.0521	$\begin{cases} 0.0286 \\ 0.0453 \\ 0.0427 \end{cases}$	$\begin{cases} 0.0205 \\ 0.0283 \\ 0.0264 \end{cases}$	11688876
(66-20-3)	0.0556	$\begin{cases} 0.0314 \\ 0.0458 \\ 0.0439 \end{cases}$	$\begin{cases} 0.0228 \\ 0.0285 \\ 0.0263 \end{cases}$	11075901
(66-66-3)	0.0546	$\begin{cases} 0.0310 \\ 0.0450 \\ 0.0453 \end{cases}$	$\begin{cases} 0.0222 \\ 0.0286 \\ 0.0279 \end{cases}$	11922921

The second challenge was to test the performances of the selected MLP structure to recognize different object positions and radii. The relative error for each parameter is shown in Fig. 5. The relative errors are quite small and do not exceed 0.6% which is satisfying result and confirms the performances of the maintained structure.

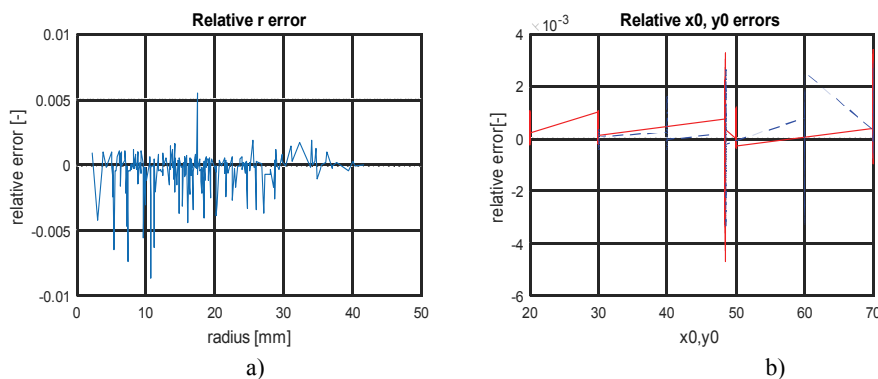


Fig. 5. Relative errors of parameters estimation in the MLP testing phase for (66-14-3) structure: a) for radius estimation, b) for coordinates' estimation: x_0 – red solid line, y_0 – blue dashed line

Further task was to test the performances of MLP in facing symmetric positions of cylindrical objects as shown in Fig. 6.

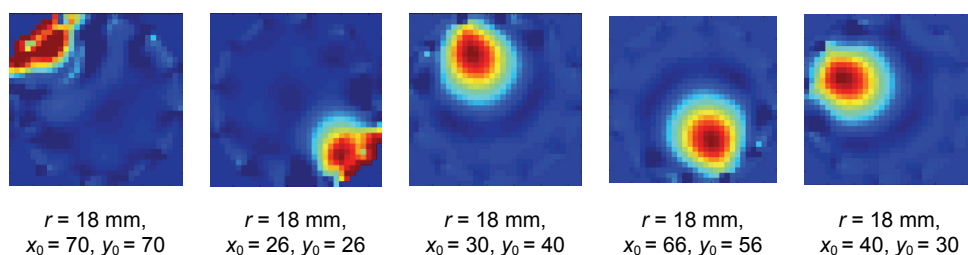


Fig. 6. Examples of different symmetric simulated phantoms used to train and test the MLP

Central symmetric coordinates of the different possible positions of the centre of the objects are calculated and new data base for different radii values were simulated. The validated structure (66-14-3) of the MLP performed the estimation of the different parameters of symmetric objects with an error of 3% (mean error) and 1% (relative error) in average for each of parameters: radius r and position (x, y) .

A second case of possible confusion when determining the coordinates of the centre of the circular shape was taken into account: Let's consider an object O_1 with centre (x_1, y_1) and O_2 with centre (x_2, y_2) where $x_2 = y_1$ and $y_2 = x_1$ which leads to O_2 with centre (y_1, x_1) . The same structure was able to differentiate the objects and shown resistance to the mentioned case of possible confusion.

The next aim of the research was to compare a speed of the proposed and traditional approaches. The elapsed time to estimate parameters using the proposed ANN based method is about 0.0005 s, which was calculated as an average of 246 measurements in the MLP testing process. This time is compared to the time of the tomographic image reconstruction (vector of permittivity distribution) by the use of two iterative methods available in the ECTsim Matlab toolbox: Linear Back Projection (LBP) and Levenberg-Marquard (LM) [25]. Time of image

processing needed to flow parameters estimation and time of image visualisation are not taken into consideration. Elapsed times and gain in computational time G for both methods and for a different number of iterations N are shown in Table 2. Results demonstrate the rapidity of the proposed ANN-based method in different studied cases. The LBP provided the faster reconstruction result than the LM but suffers from accuracy with high final image error comparing to final image error reached with the LM method.

Table 2. Elapsed times and gain on time for different iterative image reconstruction methods compared to the ANN based approach ($t_{\text{estimation}} = 0.0005$ s)

Linear back projection (LBP)			Levenberg-marquard (LM)			
$t_{\text{reconstruction}}$ [s]	G [-]	$F_{\text{image error}}$ [-]	N [-]	$t_{\text{reconstruction}}$ [s]	G [-]	$F_{\text{image error}}$ [-]
0.07	140	0.86	100	3.66	7469	0.52
			650	34.72	70851	0.2

7. Conclusions

The aim of the presented work was to determine the radius and 2D coordinates of a cylindrical structure of a flow inside a vessel using electrical capacitance tomography and artificial neural networks. ANN of MLP type with one hidden layer was applied. The proposed method has the advantages to be direct and fast. In comparison to the traditional approach applying a simple LBP algorithm the considered flow parameters are estimated by ANN 140 times faster and in comparison to the Levenberg-Marquard algorithm with 650 iterations over 70 thousand times faster (see Table 2). The relative error of parameters estimation in average is less than 1% for each of parameters: radius r and position (x, y) .

The provided results highlight the performances of the ANN-based approach to direct and fast estimation of different flow parameters from the tomographic data and thus the possibility of online cylindrical flow monitoring.

Acknowledgements

Work partially funded by the European Commission under the Erasmus Mundus GreenIT project (GreenIT for the benefit of civil society). 3772227-1-2012-ES-ERAMUNDUS-EMA21; Grant Agreement n°2012-2625/001-001-EMA2

References

- [1] Grudzien K., Romanowski A., Chaniecki Z. et al., *Description of the silo flow and bulk solid pulsation detection using ECT*, Flow Measurement and Instrumentation, vol. 21, pp. 198-206 (2010).
- [2] Zhang W., Wang C., Yang W., Wang C-H., *Application of electrical capacitance tomography in particulate process measurement – A review*, Advanced Powder Technology, vol. 25, pp. 174-188 (2014).

- [3] Jackowska-Strumillo L., Sokolowski J., Żochowski A., Henrot A., *On Numerical Solution of Shape Inverse Problems*. Computational Optimization and Applications, vol. 23, no. 2, pp. 231-255 (2002).
- [4] Isaksen Ø., *A review of reconstruction techniques for capacitance tomography*. Meas. Sci. Technol., vol. 7, pp. 325-333 (1996).
- [5] Gao R.X., Tang X., Gordon G., Kazmer D.O., *Online product quality monitoring through in-process measurement*, CIRP Annals - Manufacturing Technology, vol. 63, no. 1, pp. 493-496 (2014).
- [6] Tapp H.S., Peyton A.J., Kemsley E.K., Wilson R.H., *Chemical engineering applications of electrical process tomography*, Sensors and Actuators B: Chemical, vol. 92, no. 1-2, pp. 17-24 (2003).
- [7] Wahab Y.A., Rahim R.A., Rahiman M.H.F. et al., *Non-invasive process tomography in chemical mixtures, A review*, Sensors and Actuators B: Chemical, vol. 2, pp. 602-617 (2015).
- [8] Lei J., Liu S., Wang X., Liu Q., *An Image Reconstruction Algorithm for Electrical Capacitance Tomography Based on Robust Principle Component Analysis*, Sensors 13, pp. 2076-2092 (2013).
- [9] Lionheart W.R.B., *Developments in EIT reconstruction algorithms: pitfalls, challenges and recent development*, Review, Physiol. Meas., vol. 25, pp. 125-142 (2004).
- [10] Marashdeh Q., Warsito W., Fan L-S., Teixeira F.L., *Nonlinear Forward Problem Solution for Electrical Capacitance Tomography Using Feed-Forward Neural Network*, IEEE Sensors Journal, vol. 6, no. 2, pp. 441-449 (2006).
- [11] Kapusta P., Majchrowicz M., Sankowski D., Banasiak R., *Application of GPU parallel computing for acceleration of Finite Element Method based 3D reconstruction algorithms in Electrical Capacitance Tomography*, Image Processing & Communications, vol. 17, no. 4, pp. 343-350 (2012).
- [12] Mohamad-Saleh J., Hoyle B.S., Podd F.J.W., Spink D.M., *Direct process estimation from tomographic data using artificial neural systems*, Journal of Electronic Imaging, vol. 10, no. 3, pp. 646-652 (2001).
- [13] Romanowski A., Grudzień K., Williams R.A., *Analysis and Interpretation of Hopper Behaviour Using ECT*, Part Part. Syst. Charact. vol. 23, no. 3-4, pp. 297-305 (2006).
- [14] Wajman R., Fiderek P., Fidos H. et al., *Metrological evaluation of a 3D electrical capacitance tomography measurement system for two-phase flow fraction determination*, Meas. Sci. Technol. vol. 24, no. 065302 (2013).
- [15] Stasiak M., Sikora J., Filipowicz S.F., Nita K., *Principal component analysis and artificial neural network approach to electrical impedance tomography problems approximated by multi-region boundary element method*, Engineering Analyses with Boundary Elements, vol. 31, pp. 713-720 (2007).
- [16] Fiderek P., Wajman R., Kucharski J., *The Fuzzy System for Recognition and Control of the two Phase Gas- Liquid Flows*, Informatics Control Measurement in Economy and Environment Protection (IAPGOS), no. 4, pp. 7-11 (2015).
- [17] Ratajewicz-Mikolajczak E., Sikora J., *Neural networks method for identification of the objects behind the screen*, IEEE Trans Med Imaging, vol. 21, no. 6, pp. 613-9 (2002).
- [18] Garbaa H., Jackowska-Strumillo L., Grudzień K., Romanowski A., *Neural network approach to ECT inverse problem solving for estimation of gravitational solids flow*, In Proc. of the 2014 Federated Conf. on Computer Science and Inf. Systems, AAIA'14, vol. 2, Warsaw, Poland, pp. 19-26 (2014).
- [19] Wang H., Yang W., Proctor I. et al., *Online monitoring and flow regime identification of fluidised bed drying and granulation processes*, IST 2009 International Workshop on Imaging Systems and Techniques, Shenzhen, China (2009).
- [20] Wang C., He X., *Comparing Reconstruction Algorithms for Different Size of Object in Electrical Tomography*, 11th IEEE International Conference on Electronic Measurement & Instruments, CEMI'2013, pp. 760-764 (2013).
- [21] Liukkonen M., Hiltunen Y., Laakso I., *Advanced Monitoring and Diagnosis of Industrial Processes*, 8th EUROSIM Congress on Modelling and Simulation (2013).
- [22] Haykin S., *Neural Networks: a comprehensive foundation – 2nd ed.*, Prentice Hall (1999).

- [23] Warsito W., Fan L-S., *Development of 3-Dimensional Electrical Capacitance Tomography Based on Neural Network Multi-criterion Optimization Image Reconstruction*, Proc. of 3rd World Congress on Industrial Process Tomography (Banff), pp. 942-947 (2003).
- [24] Grudzień K., Romanowski A., Aykroyd R.G., Williams R.A., Mosorov V., *Parametric Modelling Algorithms in Electrical Capacitance Tomography for Multiphase Flow Monitoring*, IEEE, MEMSTECH'2006, Lviv-Polyana, UKRAINE, pp. 24-27 (2006).
- [25] Smolik W.T., *Accelerated Levenberg Marquardt Method With an Optimal Step Length in Electrical Capacitance Tomography*, IEEE Int. Conf. on Imaging Systems and Techniques, pp. 204-209 (2010).
- [26] ECTSim3D MATLAB's Toolbox, <http://ectsim.ire.pw.edu.pl>, accessed on April 2014.